

Boston University

OpenBU

<http://open.bu.edu>

Theses & Dissertations

Boston University Theses & Dissertations

2015

Evaluating techniques in tissue clarification using CLARITY imaging and investigating where sodium is sensed in the body

<https://hdl.handle.net/2144/16111>

Boston University

BOSTON UNIVERSITY
SCHOOL OF MEDICINE

Thesis

**EVALUATING TECHNIQUES IN TISSUE CLARIFICATION USING CLARITY
IMAGING AND INVESTIGATING WHERE SODIUM IS SENSED IN THE
BODY**

by

CHRISTOPHER MATTHEW NEAL

B.S., California State University at Long Beach, 2011

Submitted in partial fulfillment of the
requirements for the degree of
Master of Science

2015

© 2015 by
CHRISTOPHER MATTHEW NEAL
All rights reserved

Approved by

First Reader

Richard D Wainford Ph.D., FAHA
Assistant Professor of Pharmacology and Medicine

Second Reader

Hee-Young Park Ph.D.
Professor of Medical Sciences & Education and Dermatology

DEDICATION

To my family

Thanks for all the support

ACKNOWLEDGMENTS

I would sincerely like to thank Dr. Richard Wainford, Casey Carmichael and everyone else at the Whitaker Cardiovascular Institute at Boston University School of Medicine. Without their help and guidance this project would never have been possible.

**EVALUATING TECHNIQUES IN TISSUE CLARIFICATION USING CLARITY
IMAGING AND INVESTIGATING WHERE SALT IS SENSED IN THE BODY**

CHRISTOPHER MATTHEW NEAL

ABSTRACT

Objective:

Previous studies have shown the significant contribution of sympathoinhibition in response to sodium loading to prevent increases in mean arterial blood pressure in salt resistant phenotypes. It has also been shown that brain $G\alpha_{i2}$ protein gated signal transduction plays a major role in this pathway, however, the specific mechanisms through which this pathway is activated remain less well understood. The purpose of this study was to elucidate the relative contribution of increased sodium in either the plasma or the cerebrospinal fluid (CSF) to the regulation of mean arterial pressure and natriuresis. Additionally we explored the potential for using the novel CLARITY Imaging technique to identify the relative activity of neurons in areas of the brain thought to play a major role in body fluid homeostasis in response to salt.

Methods:

Rats that were pre-treated with either scrambled or $G\alpha_{i2}$ oligodeoxynucleotides (ODN), to selectively down regulate brain $G\alpha_{i2}$ proteins, were challenged either peripherally or centrally with sodium. Upon sodium loading physiological parameters were measured for two hours after which the animal's brains were recovered for immunohistochemical (IHC) analysis of the paraventricular nucleus, a known regulatory center for body fluid homeostasis and blood pressure regulation.

Additionally we adapted a version of the published CLARITY Imaging protocols for optically clearing tissue through application of electrophoretic tissue clearing (ETC) to a larger rat model.

Results:

In scrambled ODN pre-treated rats we observed a temporary increase in MAP in response to both the peripheral and central sodium challenge. In the $G\alpha_{i2}$ ODN pre-treated animals we saw some form of attenuation to this response in both studies, however, where in the peripheral challenge there was an increase in the amount of time that it took the rats to return to normotension with no alteration in natriuresis, in the central challenge there was a large attenuation in natriuresis with no differences in the time to return to baseline MAP. Our IHC analysis also showed a decrease in neuronal activation of paraventricular medial parvocellular neurons in $G\alpha_{i2}$ pre-treated rats that were challenged peripherally vs their SCR pre-treated counterparts. No such difference was observed in either of the pre-treatment groups from the central sodium challenge study.

In the CLARITY study we found that it is possible to adapt the method for optically clearing tissue to the larger model, however, we encountered several issues related to tissue swelling and peripheral tissue damage.

Conclusion:

Based on our current results it seems evident that there are at least two different mechanisms that activate the cardiovascular regulatory control centers in the brain that prevent long term increases in mean arterial pressure in response to increased salt. It also appears that these two different mechanisms are triggered either by increases in plasma or

CSF salinity, though which of these two mechanisms may be directly responsible for the development of salt sensitive hypertension requires further investigation.

While we had some success at optically clearing larger tissue volumes through ETC, problems we encountered with maintaining tissue integrity for investigations of intact neural networks prevented us from applying this technique, in its current form, to our investigation of salt sensitive hypertension.

TABLE OF CONTENTS

TITLE.....	i
COPYRIGHT PAGE.....	ii
READER APPROVAL PAGE.....	iii
DEDICATION.....	iv
ACKNOWLEDGMENTS	v
ABSTRACT.....	vi
TABLE OF CONTENTS.....	ix
LIST OF FIGURES	xiii
INTRODUCTION	1
Salt Sensitivity	1
Brain regions associated with maintaining homeostasis	3
Optical clearing of biological tissue	5
CLARITY	7
Specific Aims	8
METHODS	9
RESULTS	17
DISCUSSION.....	33
APPENDIX.....	42

LIST OF JOURNAL ABBREVIATIONS (optional)..... 43

REFERENCES 44

CURRICULUM VITAE..... 53

LIST OF FIGURES

Figure	Title	Page
1	HR and MAP in response to central sodium challenge	17
2	Cumulative sodium excretion in response to central sodium challenge	18
3	HR and MAP in response to peripheral sodium challenge	19
4	Mean number of total <i>Fos</i> ⁺ nuclei found in the PVN in response to central sodium challenge	20
5	Mean number of <i>Fos</i> ⁺ magnocellular nuclei in the PVN in response to central sodium challenge	21
6	Mean number of <i>Fos</i> ⁺ parvocellular nuclei in the PVN in response to central sodium challenge	22
7	Mean number of total <i>Fos</i> ⁺ nuclei found in the PVN in response to peripheral sodium challenge	23
8	Mean number of <i>Fos</i> ⁺ magnocellular nuclei in the PVN in response to peripheral sodium challenge	24
9	Mean number of <i>Fos</i> ⁺ parvocellular nuclei in the PVN in response to peripheral sodium challenge	25
10	Representative images of <i>Fos</i> ⁺ nuclei at level 2 of the PVN under separate experimental conditions	26

11	Rat brain N1 from trial 1 of ETC for optically clearing tissue	28
12	Rat brains N3 and N4 from trial 1 of ETC for optically clearing tissue	29
13	Rat brains N5 and N6 from trial 2 of ETC for optically clearing tissue	30
14	Rat brains N9 and N10 from trial 3 of ETC for optically clearing tissue	31
15	Rat brains N11 and N12 from trial 4 of ETC for optically clearing tissue	32

LIST OF ABBREVIATIONS

AV3V	Anteroventral Third Ventricle
CNS	Central Nervous System
CSF	Cerebrospinal Fluid
CVO	Circumventricular Organs
DP	Dorsal Parvocellular
DSS	Dahl Salt Sensitive
ETC	Electrophoretic Tissue Clearing
HR	Heart Rate
HTN	Hypertension
ICV	Intracerebroventricular
IHC	Immunohistochemistry
IML	Intermediolateral
IV	Intravenous
MAP	Mean Arterial Pressure
MnPO	Median Preoptic Nucleus
MP	Medial Parvocellular
ODN	Oligodeoxynucleotide
OVLT	Organum Vasculosum of the Lamina Terminalis
PFA	Paraformaldehyde
PM	Posterior Magnocellular
PT	Pre Treatment

PVN.....	Paraventricular Nucleus
RVLM.....	Rostral Ventrolateral Medulla
SCR.....	Scrambled
SD	Sprague Dawley
SDS	Sodium Dodecyl Sulfate
SFO	Subfornical Organ
VLP	Ventrolateral Parvocellular

INTRODUCTION

Hypertension

Hypertension, a disease that currently afflicts more than 65 million adults in the United States (11) remains one of the most elusive problems in the realm of cardiovascular health. Despite an enormous research effort around the world for several decades, the underlying mechanisms through which the complex clinical phenotype of primary hypertension develops remain poorly understood. A large body of research in this field has been directed towards the influence of salt, with an emphasis on excess dietary salt, as a potentially significant factor in the pathogenesis of hypertension (33, 45, 46). It has been repeatedly shown that increased plasma sodium can have a profound effect on both the kidneys and the components of the central nervous system related to fluid and electrolyte balance, as well as control of cardiovascular output (7, 23, 45). It has also been shown that around half of all hypertensive patients show an increase in mean arterial pressure and sympathetic nerve activity in response to salt and that among those salt-sensitive individuals there is a significantly greater incidence of developing serious cardiovascular issues and mortality (57). What is not so well understood is the specific mechanism through which salt acts to alter normal physiological functioning.

Salt sensitivity

Primary to understanding the pathogenesis of salt-sensitive hypertension is the need to understand where specifically in the body sodium is sensed. There is a substantial amount of research to support that there are several systems working

cooperatively to sense any changes in the sodium level in the plasma (7, 16, 28, 33). Systems of primary interest to the study of salt sensitive hypertension include the central nervous system (CNS), the kidneys and the sympathetic network through which they communicate. It has been shown that severing lines of communication between the CNS and the kidneys through renal denervation can attenuate the development of increased arterial blood pressure even in individuals who have been resistant to multiple different forms of therapies (50), although definitive results for the application of this method across the entire population remain elusive (5). Additional studies have shown in a rat model that ablation of the anteroventral third ventricle (AV3V) region have shown much the same attenuation in mean arterial pressure and natriuresis in response to salt as renal denervation (18, 42). Additionally lesions of the AV3V have been shown to abolish any influence of dietary salt to increasing blood pressure variability and normal cardiovascular reflexes in the salt resistant Sprague Dawley rat (42), although ablation of brain regions does not hold a great deal of promise for treatments in human beings.

It is worth noting that potential locations for the sensing of salt in addition to afferent arteriole baroreceptors of the kidneys have been found in some areas of the brain that have been associated with osmoregulation (17, 36). This complex system has created additional issues in understanding the pathogenesis of salt-sensitive hypertension given that abnormalities in the either the kidneys or the central nervous system can lead to the development of increased blood pressure (8, 26). For the

purposes of this study, the focus will be on those areas within the CNS that have been identified as likely areas for cardiovascular and osmotic regulation.

Brain regions associated with maintaining body fluid homeostasis

The areas that have been most closely linked to the development of salt sensitive hypertension can be primarily found in the forebrain lamina terminalis. These include the subfornical organ (SFO), and the organum vasculosum of the lamina terminalis (OVLT), collectively known as the sensory circumventricular organs (18). Also included are the median preoptic nucleus (MnPO) and the paraventricular nucleus (PVN). The SFO and OVLT have been shown to contain a number of sodium channels and osmo-receptors (35, 36), and their location adjoining the third ventricle and structure which allows access to both the blood as well as cerebrospinal fluid (CSF) make them likely possibilities for central sodium receptors. Additional studies have shown that projections from the CVOs are directed towards the MnPO as well as the PVN (20), sites that have been associated with summation of sensory inputs and relay stations for efferent signals to target organs and vasculature (7, 49). Several studies carried out to block sodium channels centrally or to ablate the entire region have shown a marked attenuation in the development of hypertension in the Dahl Salt Sensitive (DSS) rat when challenged with sodium (4, 22), although they do not totally stop the development of hypertension in spontaneously hypertensive rats (18).

One of the areas that has been a focus of these studies is the PVN, which is understood to be an area for the summation of sensory inputs from the sensory

organs and then a relay to those areas associated with sympathetic output such as the rostral ventrolateral medulla (RVLM) and intermediolateral cell column of the spinal cord (IML) (44). The PVN can be sub-divided into two separate groups of cells, the first group, the magnocellular neurons are thought to function primarily as endocrine cells that release , among other hormones, vasopressin (3, 49), a hormone traditionally associated with sodium and water balance. The second group of cells, the parvocellular neurons, work primarily as sympathetic-regulatory neurons projecting to endocrine control centers in the median eminence and limbic system as well as the RVLM and the IML (25). The parvocellular neurons can be further divided into the dorsal (dp), medial (mp), lateral (lp) and ventrolateral (vlp) parvocellular neurons based on their rostral-caudal position within the PVN (44) an illustration of these divisions can be found in appendix 1. It is thought that sympathetic output to the kidneys via the PVN may play a large role in the development of salt-sensitive hypertension. Studies have indicated that increased plasma sodium leads to increased activation in the CVOs (36) that then synapse with neurons within, among other regions, the PVN. PVN neurons will then go on to relay signals via the RVLM and IML to the kidneys via the renal efferent nerves. It has been shown that there is usually a sympathoinhibitory signal within the PVN which prevents too much renal sympathetic nerve activity in response to normal increases in plasma sodium associated with dietary intake. If not for this sympathoinhibition we would see a large increase in MAP after the consumption of any salt heavy meal (46, 54).

In recent years some interest has arisen as to what role G-protein coupled receptors might play in this sympathoinhibitory pathway. Early experiments from this laboratory have shown that activation of central α_2 -adrenoreceptors causes a marked diuretic and natriuretic response in concert with a decrease in both HR and MAP, however, this salt driven increase in MAP and natriuresis was blocked when animals were pre-treated with an oligodeoxynucleotide (ODN) targeted to central $G\alpha_{i2}$ proteins (52). Further studies went on to show that in addition to α_2 -adrenoreceptor activation central $G\alpha_{i2}$ proteins also play an important role in renal sympathoinhibition associated with acute volume expansion, as well as global sympathoinhibition associated with acute iso-volumetric sodium loading and chronic stressful stimuli such as a high salt diet in rats (27, 54). Additionally it was found that renal denervation eliminated any differences in groups that were pre-treated with either $G\alpha_{i2}$ or SCR ODN, from which we can infer that the $G\alpha_{i2}$ protein gated signal transduction pathway is renal nerve dependent (26).

Investigations of inter-connected neural networks through optically clearing biological tissues

One of the challenges presented by neural research is the limited ability to study intact systems. Previous techniques such as electrophysiological, pharmacological and immunohistochemistry among others, while useful are constrained by the necessity to cut the brain into many slices, which inherently severs many connections which prevents imaging of total intact systems. Systems level understanding has been the long sought golden standard through which we can hope

to fully understand not only the important components of a biological system but the manner in which they interact to allow the normal functioning of complex organisms. Whole brain imaging, with an emphasis on single cell resolution has become vital to our understanding of how certain neurological systems, such as those that regulate body fluid homeostasis, act to counter outside influences (31). Clinical issues such as hypertension tend to affect several different neural systems spread throughout the brain and understanding the manner in which these systems communicate with one another is critical to understanding the pathology of the disease. Studies such as these meet with several practical barriers including the inability to image these connections in an intact subject. Recent technological advances have begun to make it possible to study fully intact neural networks via optically clearing tissue in order to better map the connections between different areas.

A method for preparing tissue such that neurological connections can be traced within an intact specimen have long been sought after. Early discoveries such as the Golgi stain have allowed for the investigation of single-cell connection within a complex organ, however the technology necessary to view such preparations has until recently been limited by the optical constraints of light microscopy. This has been especially true within the CNS due to the high optical scattering properties of lipid membranes (10) which are highly abundant in organisms that have myelinated axons. Several different techniques have emerged for optically clearing tissue in the past utilizing a variety of chemical reagents and processes. It was initially proposed that the incubation of organic samples in chemical compounds that matched the

refractory index of the proteins and lipids of primary interest would, theoretically, render the tissue transparent under light microscopy. Early techniques for the optical clearing have used immersion in alcohols (6), urea (19), and fructose in conjunction with thiols (29) to attempt to match the refractory index of the target organs. While some measure of success was attained with these techniques several unresolved issues including tissue shrinking/swelling and fluorescent marker washout have led researchers to continue to pursue alternative methods for optically clearing tissue.

CLARITY

Clear Lipid-exchanged Acrylamide-hybridized Rigid Imaging-compatible Tissue-hydrogel (CLARITY) is a novel technique that couples the use of a rigid hydrogel perfusion in conjunction with an electrophoretic lipid clearing process to produce an optically clear tissue-hydrogel hybrid sample in which most proteins and nucleic acids remain intact and neural projections can still be identified (12, 13). This technique stands out from those previously utilized in that instead of trying to submerge tissue in a medium with a refractory index close to that of lipids, CLARITY actually removes lipid membranes leaving a much more optically clear sample. The use of acrylamide monomers and a heat activated initiator to polymerization meant that a semi-rigid lattice could be formed within cell membranes that would hold any hydrophilic molecules in place without binding any of the membrane lipids. Once this hydrogel structure is in place it then becomes possible to clear away the membrane lipids using a detergent such as SDS, leaving intact tissue that is optically clear. Using electrophoresis to push SDS micelles deep into tissue has meant that much thicker

tissue samples could be cleared than previously, allowing for the examination of many more geographically distant intact structures. Also because the majority of proteins and nucleic acids are preserved in such a sample it becomes possible to apply stains after tissue clearing meaning that any signal loss is minimized and repeated rounds of staining on any sample becomes possible.

The application of this technique to understanding the integrative role of central osmo/sodium receptors, renal afferent input as well as input from other baroreceptors that leads to the normal sympathoinhibition holds much promise in further identifying and understanding pathologies in salt sensitive populations.

Specific Aims

The specific aims of this study are three-fold.

1. The first was to examine neural activation in the hypothalamic paraventricular nucleus, as well as monitoring the diuretic, natriuretic and cardiovascular response to a central sodium load and to elucidate the significance of central $G\alpha_{i2}$ proteins in this response.
2. Secondly to examine neural activation in those same areas as well as any physiological response to acute peripheral sodium loading in animals from both SCR and $G\alpha_{i2}$ pre-treatment groups.
3. Finally to test the potential efficacy of the CLARITY imaging technique on a larger rat model, with the intention of carrying out studies on the communications between brain areas that have been associated with the maintenance of body fluid homeostasis in response to salt.

METHODS

Animals

Male Sprague-Dawley (SD) rats (Harlan Laboratories Inc., IN) weighing 275-300g were individually housed in a temperature- (range: 68-79°F) and humidity-controlled (range: 30-70%) environment under a 12-h light/dark cycle and were randomly assigned to experimental treatment groups. Rats were allowed tap water and standard rodent diet (Test Diet, St. Louis, MO, USA) *ad libitum*. All experimental protocols were approved by the Institutional Animal Care and Use Committee in accordance with the guidelines of Boston University School of Medicine and the National Institutes of Health *Guide for the Care and Use of Laboratory Animals*.

Surgical Procedures

Intracerebroventricular (ICV) cannulae implantation

Animals were anesthetized (ketamine, 30 mg/kg intraperitoneally [IP] in combination with xylazine, 3 mg/kg IP) and stereotaxically implanted with a stainless steel cannula into the right lateral cerebral ventricle 5-7 days prior to experimentation, as previously described (26, 51-54).

Acute femoral vein, artery, and bladder cannulation

On the day of the study, intracerebroventricular (ICV) scrambled (SCR) or $G\alpha_{i2}$ oligodeoxynucleotide (ODN) pretreated (PT) rats were anesthetized with sodium

methohexital (20 mg/kg IP, supplemented with 10 mg/kg intravenously [IV] as required) and instrumented with catheters in the left femoral vein, left femoral artery, and bladder for administration of an isotonic saline infusion, measurement of heart rate (HR) and arterial blood pressure (MAP), and renal function, respectively (27, 52, 54).

Experimental Protocols

Acute ICV ODN administration

Twenty-four hours prior to the day of the study, down regulation of brain $G\alpha_{i2}$ protein expression levels in rats was achieved by ICV injection (25 $\mu\text{g}/5\mu\text{l}$ delivered over 60- sec) of a phosphodiesterase ODN probe dissolved in isotonic saline that selectively targets $G\alpha_{i2}$ proteins (5'-CTT GTC GAT CAT CTT AGA-3') (27, 51, 54). Control studies involved ICV injection of a SCR ODN (5'-GGG CGA AGT AGG TCT TGG-3') (The Midland Certified Reagent Company Inc., Midland, TX, USA). An NCBI Basic LocalAlignment Search Tool search of the *Rattus norvegicus* RefSeq protein database was conducted to confirm the specificity of the $G\alpha_{i2}$ ODN for the rat $G\alpha_{i2}$ protein sequence and that the SCR ODN does not match any known rat protein sequence. Multiple publications from our laboratory have confirmed effective (~85%) ODN-mediated down regulation of $G\alpha_{i2}$ protein expression in the acute setting as assessed by Western blotting (26, 51-54). This was not carried out in the current study since the tissue processing required for immunohistochemical analysis rendered the tissue unusable for western blotting.

Acute central sodium challenge

Following femoral vein, artery, and bladder cannulation (as outlined above), rats were placed in a Plexiglas holder and an IV infusion of isotonic saline (20 μ l/min) was maintained for a 2-h surgical recovery period prior to experimentation to enable the animal to regain full consciousness and for cardiovascular and renal excretory functions to stabilize. HR and MAP were continuously recorded via the surgically implanted femoral artery cannula using computer-driven BIOPAC data acquisition software (MP150 and AcqKnowledge 3.8.2, Goleta, CA, USA) connected to an external pressure transducer (P23XL; Viggo Spectramed Inc., San Francisco, CA, USA) (27, 52, 54). Following the 2-h recovery period, baseline HR and MAP were recorded continuously over a 20-min control period in conscious rats. After measurement of baseline parameters, animals received a central sodium challenge: ICV injection of 5 μ L of 1M NaCl over 30 seconds (42) and changes in HR and MAP were continuously recorded for 120-min and urine was collected in 10-min increments for the duration of the experiment (N=4/treatment group/time point).

Acute peripheral sodium challenge

Following femoral vein, artery, and bladder cannulation and recovery (as outlined above), baseline HR and MAP were recorded continuously over a 20-min control period in conscious rats. After measurement of baseline parameters, animals received a peripheral sodium challenge: IV bolus dose of 3M NaCl (0.14 ml/100g

delivered over 30-sec) (4) and changes in HR and MAP were continuously recorded for 120-min and urine was collected in 10-min increments for the duration of the experiment (N=6/treatment group/time point)

Central Nervous System Tissue Collection

Following completion of the acute sodium challenge protocol, rats were deeply anesthetized with sodium methohexital (10 mg/kg IV) and immediately perfused transcardially with 0.2-0.3 L of 0.1M phosphate-buffered saline (PBS) followed by 4% paraformaldehyde (PFA) in 0.1M PBS (4°C, 0.3-0.5 L). The brains were removed and placed in a vial containing 4% PFA in PBS overnight and then switched to a 30% w/v sucrose solution for two days (41). The PVN was sectioned into three separate sets of serial 40- μ m coronal sections that were collected into a cryoprotectant [30% sucrose +30% ethylene glycol + 1% polyvinyl-pyrrolidone in 0.1M PBS] and stored at -20°C until they were processed for immunohistochemistry.

Fos Immunoreactivity and Histological Analysis

Free-floating sections from each brain were processed for rabbit polyclonal anti-Fos antibody (Calbiochem, San Diego, CA, USA) as previously described (41). Briefly, sections were brought to room temperature and rinsed twice for 30-min in 0.1M PBS to remove cryoprotectant. Sections were incubated in 0.3% hydrogen peroxide in distilled water for 30-min at room temperature then rinsed for 30-min in 0.1M PBS. Sections were then incubated for 2-h at room temperature in PBS diluent

[3% normal horse serum in 0.1M PBS containing 0.25% Triton-100 (Sigma- Aldrich, St. Louis, MO, USA)]. The rabbit polyclonal anti-Fos antibody was diluted to 1:30,000 in PBS diluent and the sections were incubated in the primary antibody for 48- h at 4°C. After two 30-min rinses in 0.1M PBS, sections were incubated in a biotinylated horse anti-rabbit IgG (Vector Laboratories, Burlingame, CA, USA) diluted to 1:200 in PBS diluent for 2-h at room temperature. The tissue was reacted with an avidin peroxidase conjugate (ABC-Vectastain kit; Vector Laboratories, Burlingame, CA, USA) and PBS containing 0.04% 3,3'-diaminobenzidine hydrochloride and 0.04% nickel ammonium sulfate (Sigma-Aldrich, St. Louis, MO, USA). Sections were mounted on gel coated slides, processed through a series of dehydrating alcohols followed by xylenes, and placed under a coverslip with Permount mounting medium. Tissue sections were analyzed using an Olympus microscope (BX41) equipped for epifluorescence and an Olympus DP70 digital camera with DP manager software (v2.2.1). The PVN was identified using the stereotaxic atlas of Paxinos and Watson (40) and sampled at three rostral-caudal levels, as previously described (44) see illustration in appendix. Care was taken to ensure that the sections used were from the same rostral-caudal plane in each brain. Analysis was performed on two sets of tissue for each animal. The number of Fos-positive cells were visually quantified by participants blind to the experimental conditions using National Institutes of Health ImageJ software and the counts for the total PVN and each subnucleus were averaged for each animal.

Analytical Techniques

Analysis of Urine

Urine volume was determined gravimetrically assuming 1g = 1ml. Urinary Sodium was measured using a flame photometer (model: 943, Instrumentation Laboratory, Bedford, MA, USA) (26, 27, 51, 52, 54).

Statistical Analysis

Results are expressed as mean \pm SEM. The magnitude of changes in cardiovascular and renal excretory parameters at different time points after ICV sodium challenge were compared with respective group control values by a one-way repeated-measures (RM) ANOVA with a subsequent Dunnett's multiple comparison test (GraphPad Prism v. 6.00 for PC OS; GraphPad Software, San Diego, CA, USA). For consistency the same controls were used for all parts of the experiment. Differences occurring between treatment groups were assessed by a two-way RM (mixed model) ANOVA (treatment x time). The time (minutes) was the repeated factor and post hoc analysis was performed using the Bonferroni's post-test. The number of Fos positive cells in each subregion of interest was compared with respective group control values by a one-way RM ANOVA and between groups by a two-way RM ANOVA with a subsequent Dunnett's multiple comparison test and Bonferroni's post-test, respectively.

In each case, statistical significance was defined as $P < 0.05$.

Clarity

Hydrogel

Animals were deeply anesthetized with sodium methohexital (20 mg/kg IP) and immediately perfused transcardially with 75-80mL of 4°C hydrogel solution (4% paraformaldehyde, 4% Acrylamide in a 0.1M PBS solution with an additional 0.05% Bismuth buffer and 0.25% VA-044 heat activated Initiator). After perfusion the brains were recovered and placed into cold hydrogel solution where they were stored at 4°C for seven days (12).

De-gassing

After seven days the samples were degassed in a desiccation chamber where oxygen was removed and nitrogen gas was introduced. After degassing the samples were placed in a 37°C water-bath for four hours during which time the acrylamide monomers polymerized into a gelatinous matrix.

Clearing

After polymerization occurs the additional hydrogel was gently pulled away from the tissue using gloved hands, and then the brain was placed into a clearing solution (dH₂O, 4% Sodium Dodecyl Sulfate, and NaOH pellets to pH 8.5). After three days during which time additional hydrogel is dialyzed from the tissue, the brains were placed into a specially constructed electrophoresis chamber connected to a

water circulator circulating clearing solution heated to 37°C, electrophoresis was run at 30V over five days. After five days the tissue was removed from the electrophoresis chamber and rinsed in 0.1M PBS with 0.1% Triton after which it was placed into a solution of focus clear (CelExplorer labs Co., Hsinchu, Taiwan) (12).

RESULTS

Effects of central sodium challenge on cardiovascular and renal excretory function

Following 5 μ L 1M NaCl ICV injection no difference in peak bradycardia (ICV 1M NaCl Δ HR [bpm]; SCR: -24 ± 16 vs. $G\alpha i_2$: -37 ± 15 , $P>0.05$) (**Fig 1A**) or peak change in mean arterial pressure (MAP) was observed between the two groups (ICV 1M NaCl Δ MAP [mmHg] SCR: $+6\pm 3$ mmHg vs. $G\alpha i_2$: $+10\pm 2$, $P>0.05$). In both treatment groups MAP returned to baseline values within 120 min of treatment (MAP 120-min post NaCl [mmHg] SCR: 126 ± 2 vs. $G\alpha i_2$: 129 ± 2 , $P>0.05$) (**Fig 1B**).

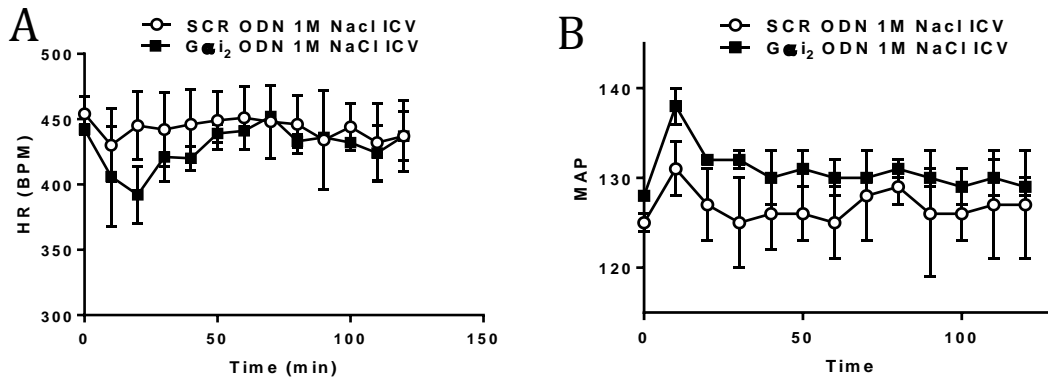


Fig. 1 **A** Heart rate (BPM) response to 1M NaCl ICV injection (5 μ L) in conscious male SD rats pretreated ICV with a SCR or $G\alpha i_2$ ODN (25 μ g/5 μ L) (N=4/group). Data are mean \pm SEM (N=4/group). **B**. Mean arterial pressure (mmHg) in response to 1M NaCl ICV injection (5 μ L) in conscious male SD rats pretreated ICV with a SCR or $G\alpha i_2$ ODN (25 μ g/5 μ L). Data are mean \pm SEM (N=4/group).

Cumulative sodium excretion was significantly greater in the SCR PT group compared to the $G\alpha_{i2}$ PT group over the course of the 120 minutes (**Fig 2**).

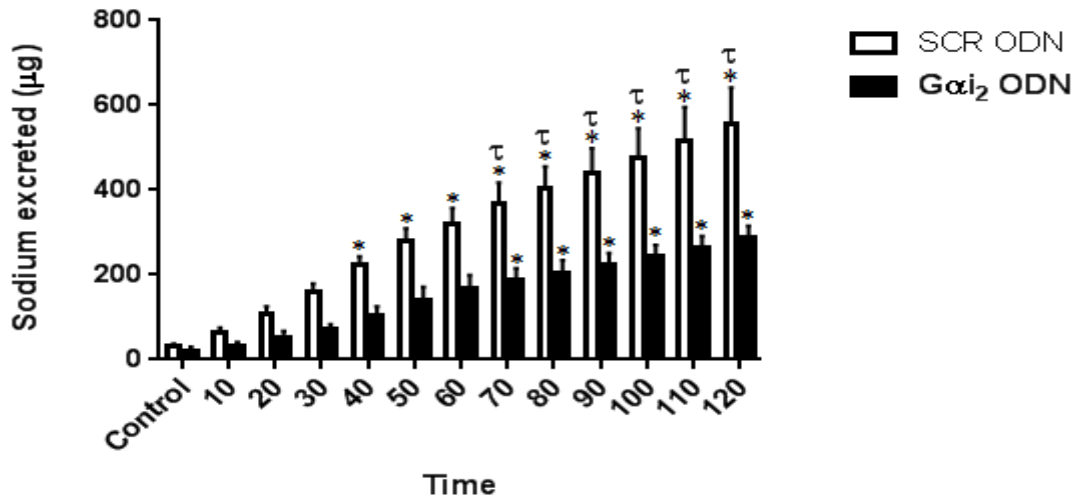


Fig. 2. Cumulative sodium excretion in response to 1M NaCl ICV injection (5 μ L) in conscious male SD rats pretreated ICV with a SCR or $G\alpha_{i2}$ ODN (25 μ g/5 μ L) (N=4/group). Data are mean \pm SEM (N=4/group). *P < 0.05, sig. diff vs. respective control value, τ P < 0.05, sig. diff. vs. respective SCR ODN value.

Effect of peripheral sodium challenge on cardiovascular and renal excretory parameters

Following IV bolus sodium challenge in male SD rats PT with a $G\alpha_{i2}$ - or SCR ODN, peak bradycardia was significantly greater in SCR animals as compared to $G\alpha_{i2}$ animals (IV 3M NaCl Δ HR [bpm]; SCR: -79 ± 15 vs. $G\alpha_{i2}$: -59 ± 12 , $P < 0.05$). No difference was observed in peak changes in MAP (IV 3M NaCl Δ MAP [mmHg] SCR: $+17 \pm 4$ mmHg vs. $G\alpha_{i2}$: $+13 \pm 3$, $P > 0.05$). In SCR PT rats, MAP returned to baseline by 100-min whereas in $G\alpha_{i2}$ PT rats MAP remained significantly elevated (MAP 100-min post NaCl [mmHg]

SCR: 134 ± 2 vs. $G\alpha i_2$: 146 ± 3 , $P < 0.05$) (**Fig. 3**). There was no observable difference in any renal excretory parameters between the two groups (data not shown).

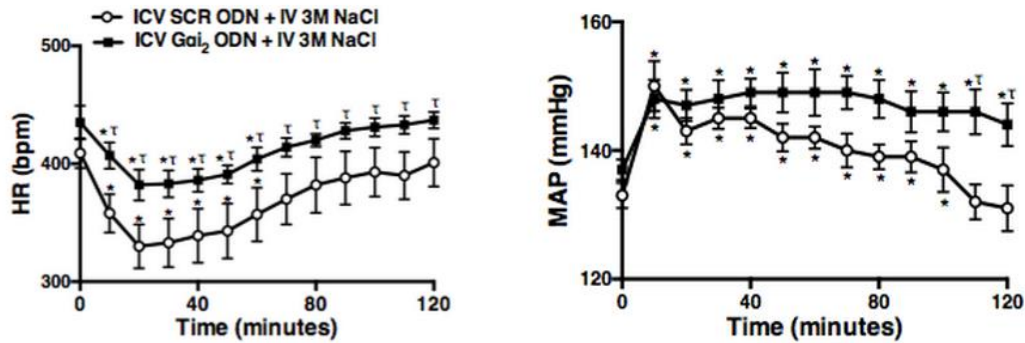


Fig. 3. **A** Heart rate (BPM) and **B.** MAP (mmHg) responses produced by 3M NaCl IV bolus (0.14 mL/100g) in conscious male SD rats pretreated ICV with a SCR or $G\alpha i_2$ ODN (25 μ g/5 μ L) (N=8/group). Data are mean \pm SEM (N=8/group). * $P < 0.05$, sig. diff. vs. respective control value, $\tau P < 0.05$, sig. diff. vs. respective SCR ODN value.

Effects of central sodium challenge on Fos production within the PVN

The total number of Fos-positive (Fos⁺) cells was not significantly different at control between treatment groups ([PVN Fos⁺ cells] SCR: 17 ± 1 vs. $G\alpha i_2$ control: 14 ± 2 , $P > 0.05$). By 120-min, the level of Fos⁺ cells in both groups were significantly greater than their respective control levels, with no significant difference in activation between the two groups ([PVN Fos⁺ cells] SCR: 97 ± 10 vs. $G\alpha i_2$ 120 min: 99 ± 10 , $P > 0.05$) **Fig 4**. Due to the absence of a difference between the two groups we chose to observe only one time point at 120 min, at which point the animals had returned to baseline MAP and HR.

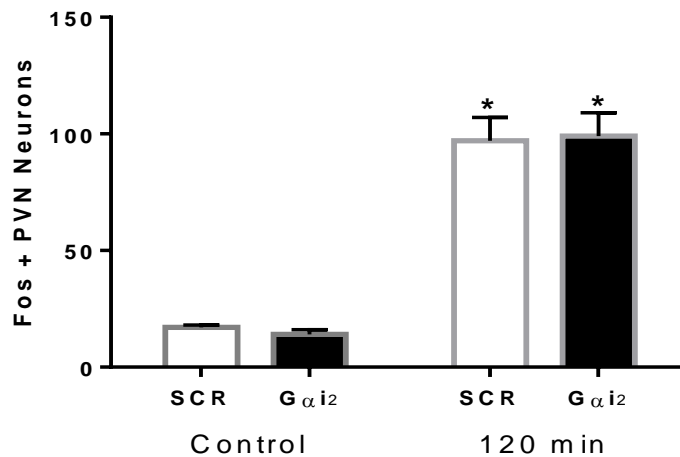


Fig. 4. Mean number (per section) \pm SEM of total PVN *Fos*⁺ nuclei in ICV SCR ODN- or *G α i₂* ODN- pre-treated male SD rats at control, and 120 min post ICV NaCl administration (N=3/group/time point). *P<0.05, sig. diff. vs. respective control value.

Effects of central sodium challenge on Fos production in PVN magnocellular neurons

PVN Fos immunoreactivity was further analyzed by subnuclei whose cytoarchitectonic boundaries were determined based on the rostral-caudal level of each section (44). The total number of Fos⁺ magnocellular neurons (i.e., posterior magnocellular [PM]) was significantly greater at 120-min post-NaCl administration as compared to control in both SCR and *G α i₂* PT groups ([PM Fos⁺ cells] SCR control: 3 \pm 1 vs. 120-min post-NaCl: 13 \pm 2; *G α i₂* control: 2 \pm 0 vs. 120-min post-NaCl: 15 \pm 3, P<0.05). There were no significant differences between SCR and *G α i₂* PT groups at any time point (**Fig. 5**).

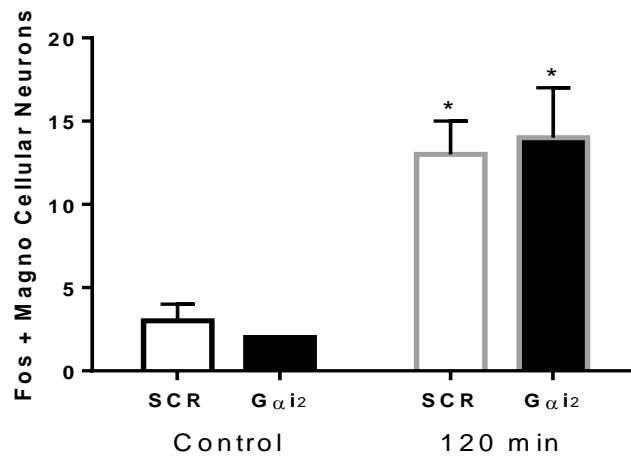


Fig 5. Mean number (per section) \pm SEM of total PVN Magnocellular *Fos*⁺ nuclei in ICV SCR ODN- or *Gai*₂ ODN- pre-treated male SD rats at control, and 120 min post ICV NaCl administration (N=3/group/time point). *P<0.05, sig. diff. vs. respective control value.

Effect of central sodium challenge on Fos immunoreactivity in PVN parvocellular neurons

PVN parvocellular neurons were further analyzed as dorsal (DP), medial (MP), and ventrolateral (VLP) subregions based on the respective rostral-caudal level of the PVN. No differences between the PT groups in the number of Fos⁺ nuclei were observed in any parvocellular subregions prior to sodium challenge ([DP Fos⁺ cells] SCR control: 4 \pm 0 vs. *Gai*₂ control: 4 \pm 0, P>0.05, [MP Fos⁺ cells] SCR control: 8 \pm 1 vs. *Gai*₂ control: 6 \pm 1, P>0.05, [VLP Fos⁺ cells] SCR control: 5 \pm 1 vs. *Gai*₂ control: 4 \pm 1, P>0.05). At 120-min, both SCR and *Gai*₂ PT rats exhibited significant increases in DP, MP, and VLP regions as compared to control but no significant differences between treatment groups ([DP Fos⁺ cells] SCR 120 min: 15 \pm 3 vs. *Gai*₂ 120 min: 13 \pm 2, P<0.05,

[MP Fos⁺ cells] SCR 120 min: 60±3 vs. Gαi₂ 120 min: 54±6, P<0.05, [VLP Fos⁺ cells] SCR 120 min: 16±3 vs. Gαi₂120 min: 23±3, P<0.05) **Fig 6.**

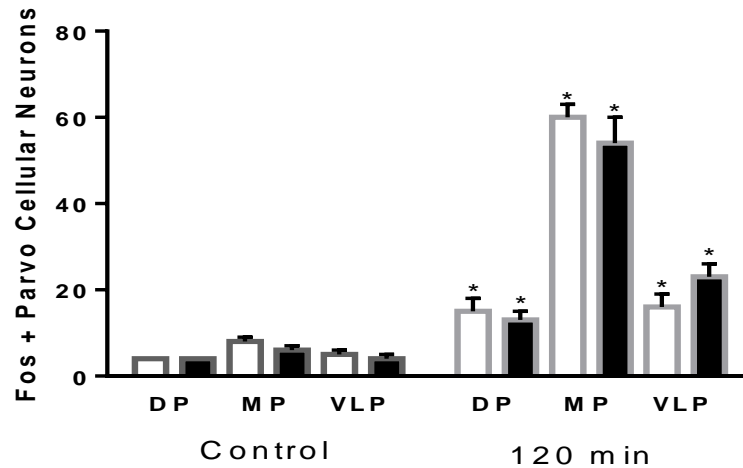


Fig 6. Mean number (per section) ± SEM of total PVN Parvocellular Fos⁺ nuclei in ICV SCR ODN- or Gαi₂ ODN- pre-treated male SD rats at control, and 120 min post ICV NaCl administration (N=3/group/time point). *P<0.05, sig. diff. vs. respective control value

Effect of peripheral sodium challenge on total PVN Fos immunoreactivity

The total number of Fos⁺ cells was not significantly different at control between treatment groups, for the purpose of continuity the same controls were used for both the central as well as peripheral sodium challenges ([PVN Fos⁺ cells] SCR: 17±1 vs. Gαi₂ control: 14±2, P>0.05). At 40-min post-NaCl administration, a significant increase in Fos immunoreactivity was observed in SCR, but not Gαi₂ PT rats ([PVN Fos⁺ cells] SCR control: 17±1 vs. 40-min post-NaCl: 52±5, P<0.05; Gαi₂ control: 14±2 vs. 40-min post-NaCl: 30±6). Gαi₂ PT rats also displayed significantly less Fos⁺ nuclei compared to the respective SCR PT rats ([PVN Fos⁺ cells] SCR 40-min post-NaCl: 52±5 vs. Gαi₂ 40-min post-NaCl: 30±6, P<0.05). By 100-min, the level of Fos positive cells in both groups were

significantly greater than their respective control levels, yet $G\alpha i_2$ PT rats continued to display significantly less Fos^+ nuclei compared to their respective SCR PT group value ([PVN Fos^+ cells] SCR 100-min post- NaCl: 107 ± 14 vs. $G\alpha i_2$ 100-min post-NaCl: 65 ± 10 , $P < 0.05$) **Fig 7**.

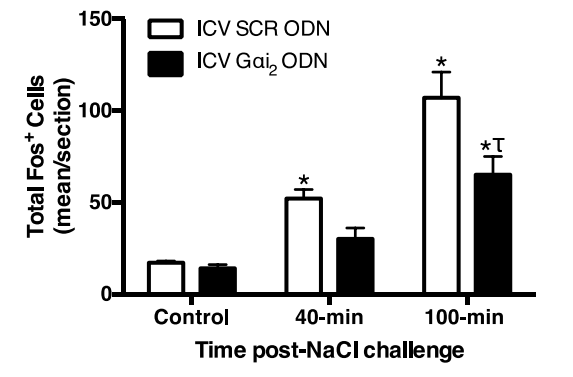


Fig 7. Mean number (per section) \pm SEM of total PVN Fos^+ nuclei in IV SCR ODN- or $G\alpha i_2$ ODN- pre-treated male SD rats at control, 40 min and 100 min post IV NaCl administration (N=8/group/time point). * $P < 0.05$, sig. diff. vs. respective control value. $\tau P < 0.05$, sig. diff. vs respective SCR ODN

Effect of peripheral sodium challenge on Fos immunoreactivity in PVN magnocellular neurons

The total number of Fos^+ magnocellular neurons (*i.e.*, posterior magnocellular [PM]) was significantly greater at 100-min post-NaCl administration as compared to control in both SCR and $G\alpha i_2$ PT groups ([PM Fos^+ cells] SCR control: 3 ± 1 vs. 100-min post-NaCl: 31 ± 5 ; $G\alpha i_2$ control: 2 ± 0 vs. 100-min post-NaCl: 26 ± 4 , $P < 0.05$). There were no significant differences between SCR and $G\alpha i_2$ PT groups at any time point. **Fig 8**.

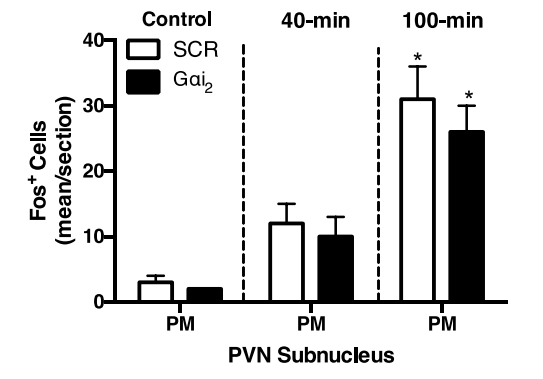


Fig 8. Mean number (per section) \pm SEM of total PVN Magnocellular *Fos*⁺ nuclei in IV SCR ODN- or *Gai*₂ ODN- pre-treated male SD rats at control, 40 min and 100 min post ICV NaCl administration. * $p < 0.05$ sig. diff. vs respective control value.

Effect of peripheral sodium challenge on Fos immunoreactivity in PVN parvocellular neurons

No differences between the PT groups in the number of *Fos*⁺ nuclei were observed in any parvocellular sub regions prior to sodium challenge. At 40 min, acute sodium challenge significantly increased Fos immunoreactivity in the MP region in the SCR PT group ([MP *Fos*⁺ cells] SCR control: 8 ± 1 vs. 40-min post-NaCl: 29 ± 4 , $P < 0.05$), while no differences in any region were observed in the *Gai*₂ PT group as compared to respective control levels. At 100-min, SCR PT rats exhibited significant increases in DP, MP, VLP, and LP regions as compared to control. As compared to *Gai*₂ PT rats, SCR PT rats exhibited significantly more *Fos*⁺ cells in MP, VLP, and LP regions (**Fig 9**).

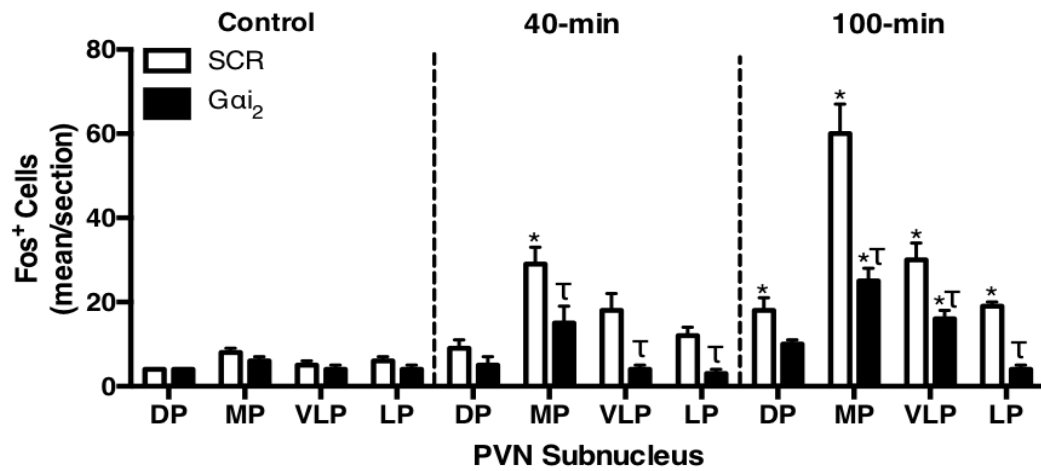


Fig 9. Mean number (per section) \pm SEM of total PVN Parvocellular *Fos*⁺ nuclei in ICV SCR ODN- or *Gai*₂ ODN- pre-treated male SD rats at control, 40 min and 100 min post IV 3M NaCl administration (N=8/group/time point). *P<0.05, sig. diff. vs. respective control value. τ P<0.05, sig. diff. vs respective SCR ODN

Fig 10.

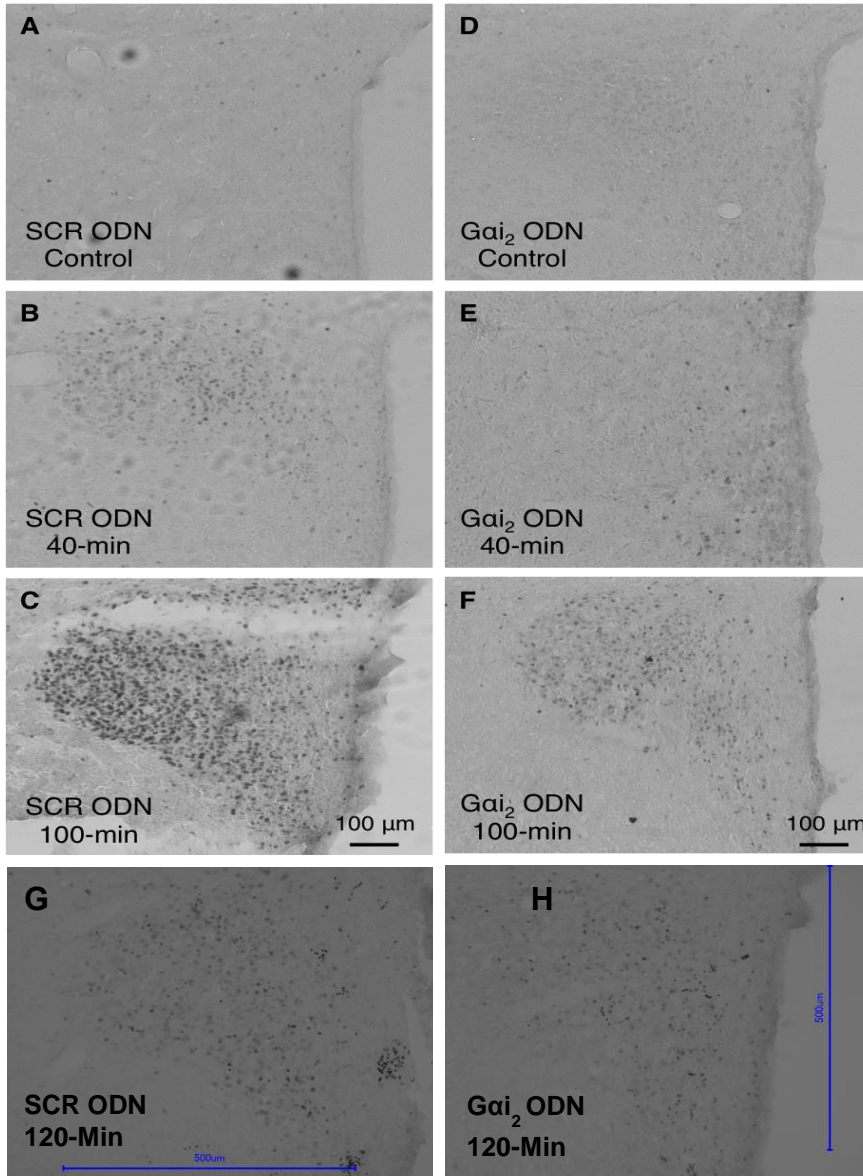


Fig 10. Representative images of total PVN Fos-positive nuclei at level 2 in ICV SCR ODN- (A-C) or Gai₂ ODN- (D-F) pretreated male SD rats at control, 40-min, and 100-min post- peripheral sodium challenge. PVN Fos-positive nuclei at level 2 in ICV SCR ODN (G), or Gai₂ ODN (H) at 120-min post central sodium challenge.

Clarity

Trial 1

In order to accommodate for the larger size of the animals used (i.e., Rats vs. Mice) some minor changes were made to the initial experimental protocol (12). The initial perfusions were carried out according to the initial protocol, though a greater amount of Hydrogel was used; 75mL at a perfusion rate of 100 RPMs. The samples were stored in 35mL of hydrogel at 4°C for 8 days prior to degassing. After degassing and nitrogen addition all samples were placed in a water bath at 37°C for 4 hours to allow polymerization to occur. Post polymerization the samples were removed from the hydrogel matrix and placed into clearing solution for a total of 7 days, additional time of 4 days was included prior to electrophoretic tissue clearing (ETC) in order to account for increased size of specimens [Original protocol specifies at least 3 days (12, 13)]. ETC was begun for samples N1 and N2 7 days post degassing at an original temp of 40°C and voltage of 15V. After 3 days of ETC samples were removed from chambers and examined, clearing was seen in much of the outer cortex however some physical trauma was observed in the already cleared tissue. In order to minimize damage to cleared tissue the samples were removed from the IHC chambers that had been holding them in place within the ETC chamber. At this time due to equipment constraints, voltage of electrophoresis was turned down to 10V for the remainder of run, all additional samples were run using a power source that allowed for significantly higher current. Samples were run for an additional 3 days at 10V and 40°C. Upon removal from ETC it was discovered that specimen N2 had been mostly

dissolved, this is thought to be from constant abrasive action of moving fluid and limited protection from movement within the chamber. Sample N1 had a strong degree of clearing with only some parts of the mid brain remaining opaque, physical trauma to the outer cortex were noted although the general structure was preserved well. In both samples a large amount of swelling was observed. **Fig 11.**

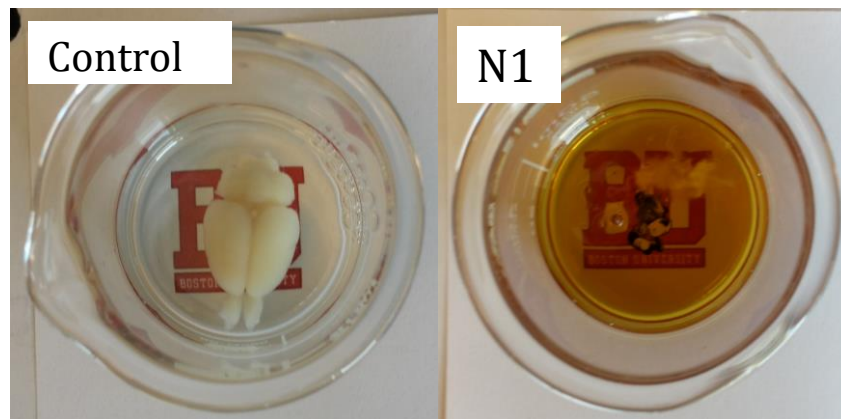


Fig 11. Rat brain prior to ETC treatment. Right hemisphere rat brain treated with Clarity Imaging Technique

Samples N3 and N4 were begun on ETC 14 days post degassing at 37° and 30V. In order to prevent continuing external trauma samples were sealed into small mesh bags, N3 was clipped in using a staple, N4 was sewn in with silk sutures. ETC for this stage was inconsistent due to failure in one of the chambers, so sample N4 was placed back into clearing solution at 20°C for holding. Sample N3 was placed into functioning chamber and begun at highest recommended electrophoresis setting of 50°C at 60V. After 3 days sample was removed from ETC chamber and was found to be burnt beyond recognition leaving only some black remnants, burning thought to be due to

contact of the staple with either of the chamber electrodes when the specimen shifted within the chamber. Due to result destruction of sample N3 all potentially conductive equipment was removed from ETC setup and sample N4 was begun at 50°C and 60V. After 3 days specimen showed initial signs of clearing in the outer cortex however burning was also occurring along one side so additional ETC was discontinued **Fig 12**.

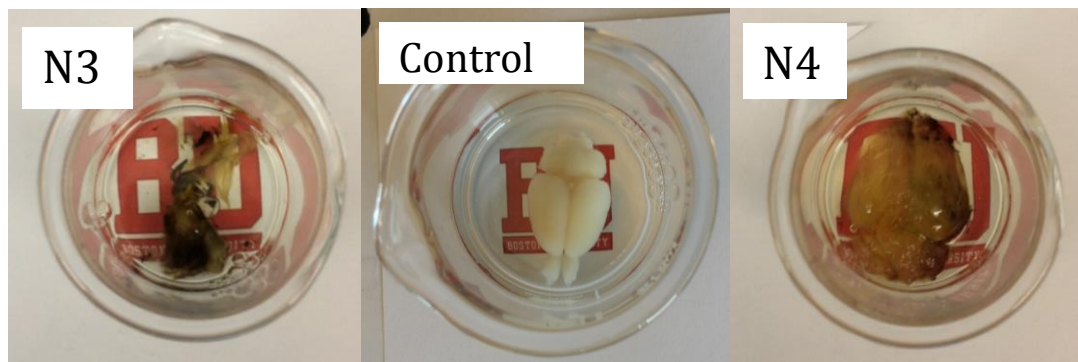


Fig 12. N3 and N4 rat brains treated with electrophoretic tissue clearing, for CLARITY Imaging

Trial 2

Animals N5 and N6 were perfused with 75mL of Hydrogel (4°C) for 10 min at 85rpm. After perfusion samples were left in additional 35mL hydrogel and stored for 7 days (4°C). After 45 min under a vacuum (-.01 atm) and addition of nitrogen gas samples were placed into a 37°C water bath for 4 hours and then placed into clearing solution at 20°C for 7 days. Samples were placed into IHC cell strainers that were sewn together to minimize tissue movement and to prevent contact with electrodes. ETC was run at 37°C and 30V for 7 days, with clearing solution changed after 3 days,

after which samples were removed and rinsed in 0.1M PBST 3x before finally being placed in Focus clear solution **Fig 13**. The best result was seen in sample N6 which was almost entirely transparent, sample N5 was almost as clear though some opaque tissue remained in the mid brain. While clearing was remarkably increased in these samples there was still a large degree of swelling.

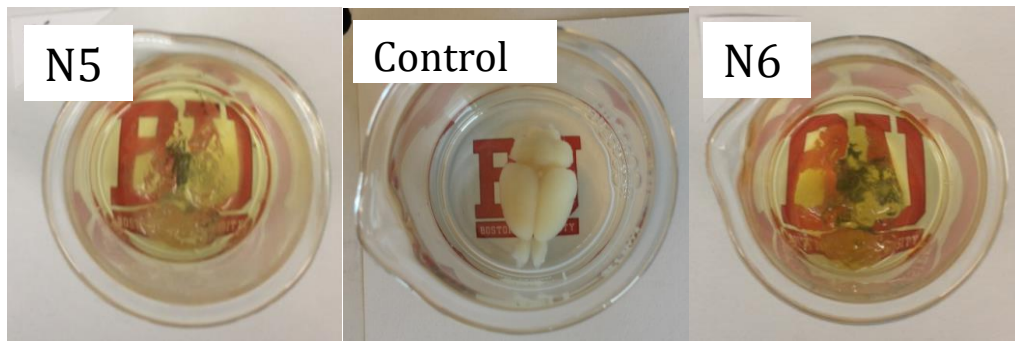


Fig 13. N5 and N6 rat brains treated with electrophoretic tissue clearing, for CLARITY

Trial 3

Samples N9 and N10 were perfused and degassed following the protocol established in trial 2. After polymerization specimens were placed into clearing solution at 20°C for 7 days. Both samples were placed into IHC cell strainers and sewn in as in trial 2 and ETC was begun at 50°C and 60V. After 3 days samples were removed from ETC and examined **Fig 14**. A large degree of clearing was observed, however a much greater degree of damage to the outer cortical layers was also seen, this effect was contributed to the combined stresses of heat and current.

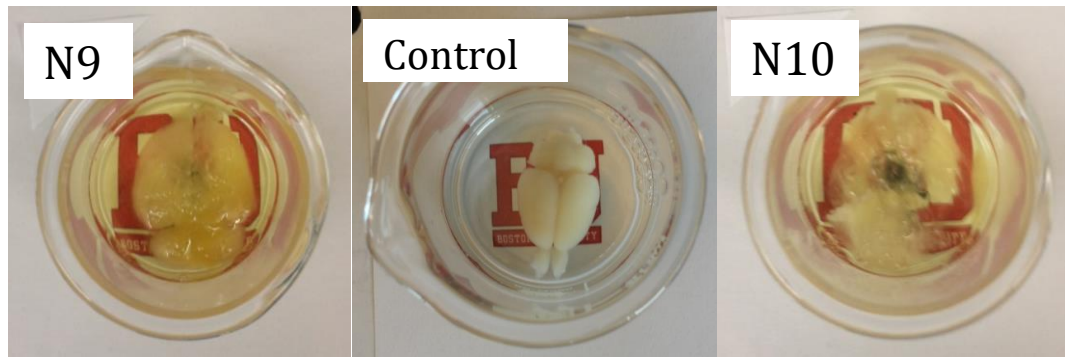


Fig 14. N9 and N10 rat brains treated with electrophoretic tissue clearing, for CLARITY

Trial 4

Samples N11 and N12 were perfused, degassed and held in clearing following protocol established in trial 2. After 7 days in clearing solution samples were placed in ETC chambers and run at 20°C and 45V. It was hoped that the decreased temp might limit the amount of tissue swelling. After three days some clearing was observed though markedly less than trials 2 and 3, with about the same amount of external damage **Fig 15.**



Fig 15. N11 and N12 rat brains treated with electrophoretic tissue clearing, for CLARITY

Discussion

These acute studies were intended to show the effect of a central vs peripheral increase in sodium on cardiovascular and renal regulation of mean arterial pressure and natriuresis. Where the peripheral study was primarily concerned with increases in plasma sodium, the central study was aimed at eliminating alterations in plasma sodium so as to elucidate the relative contributions of the central nervous system to an acute sodium challenge. Both pre-treatment groups (SCR or $G\alpha_{i2}$ ODN) in the central sodium study showed the increase in MAP that is characteristic of a central sodium challenge (22, 46), however the natriuretic response in the $G\alpha_{i2}$ group was significantly attenuated. This is consistent with the observation that the reductions in sympathetic outflow in response to sodium loading is at least partially mediated by central nervous system $G\alpha_{i2}$ protein gated signal transduction pathways (54). It was found when we challenged SCR and $G\alpha_{i2}$ pre-treated animals peripherally with 3M NaCl that there was an increase in time to return to normotension in the $G\alpha_{i2}$ animals vs their SCR counterparts. These observations serve to extend previous research from this laboratory that has shown an endogenous up-regulation of $G\alpha_{i2}$ proteins within the PVN in response to chronic high salt intake and is required for maintaining normotension (26, 27). Interestingly while both the 1M NaCl ICV and 3M NaCl IV challenges showed some sort of attenuated response in the $G\alpha_{i2}$ pre-treatment group, the response in the central challenge was related to natriuresis while the peripheral response was concerned with MAP. These results potentially illustrate two separate

mechanisms through which the body senses and then responds to increased sodium levels in either the CSF or the plasma.

There is significant evidence in support of the subfornical organ (SFO) and the organum vasculosum of the lateral terminalis (OVLT) as the primary sensory organs responsible for changes in salt concentration and osmolarity within the central nervous system. Studies have shown a significant endogenous increase in the production of the *Fos* protein, a classical indicator of neural activity, in the CVOs in response to sodium loading or dehydration (39, 44). Additional studies have identified the presence of numerous different sodium channels including a disproportionate expression of ENaC channels within the SFO and OVLT (1, 35, 36). A Na_x channel that has been shown to be sodium level sensitive has also been identified within the sensory CVOs (55). It has also been shown that an endogenous increase in *Fos* production within the CVOs that have shown an increased expression of ENaC, under an acute sodium infusion (36). It is interesting to note that both the SFO and OVLT lack a true blood brain barrier (17) and are therefore ideally situated to monitor sodium concentration in both the plasma and CSF. This cyto-architectural feature also presents an interesting question as to whether CSF, or plasma sodium, or a combination of the two is the primary force behind increased or decreased sympathetic output in response to higher or lower sodium values. No current studies have yet been able to definitively show whether it is increases in sodium or osmolarity in the CSF or the plasma that has a greater effect on the cells within this area.

Our new data as well as previous studies have shown that cardiovascular alterations in response to sodium are dose dependent in both peripheral and central sodium challenges (22, 54). The ablation of the entire AV3V region in the dahl salt sensitive (DSS) rat has been shown to attenuate or abolish increases in mean arterial pressure in response to both chronic high salt intake and acute sodium challenges (46), although hypertension has been shown to still develop in spontaneously hypertensive rats even after the AV3V was lesioned (18). Studies in Sprague Dawley rats with chronic AV3V lesions on either a high or low salt diet have shown a near abolishment in any altered responses between dietary groups to central sodium loading that had previously been seen in animals with an intact AV3V on a high vs low salt diet (42). This evidence supports the argument that ablation of the AV3V may well attenuate the development of salt sensitive hypertension, although somewhat impractical as a treatment option for humans.

The results of our current immunohistochemical analysis demonstrated that there was no difference in the pre-treatment groups at control in terms of neuronal activity. After the administration of central sodium we found significantly increased levels of *Fos* expression in the PVN. These results confirm previous findings that higher sodium levels correspond to increased *Fos* production in this cardiovascular regulatory control center of the brain (36). Previous research has also shown increased *Fos* production in the SFO, OVLT, SON, and MnPO in response to increased sodium (41), as well as an increased sensitivity to salt in animals that are on a chronic

high salt diet (44). This increase in sensitivity is generally manifested as an increase in sympathetic nerve activity in response to a sodium load vs an animal that has not been on a chronic high salt diet, which is suggestive of a change in the way that salt is sensed over time (42). Additional results from this study have shown a significant difference in *Fos* production within the parvocellular neurons of the PVN between the two PT groups when challenged peripherally with 3M NaCl I.V. bolus, with a marked attenuation in *Fos* production in the PT group that lacked functional $G\alpha_{i2}$ proteins. We have also noted that the $G\alpha_{i2}$ pre-treated animals recovery time to normotension was significantly attenuated after peripheral sodium treatment. It is possible that this delayed return to normotension could result in consecutive salt loads, as could be expected by frequent high salt meals, leading to a slow progressive increase in MAP due to having not recovered to normal levels prior to the next salt load. These findings could illustrate a potential pathway for the pathogenesis of salt sensitive hypertension in human beings. Identification of such a pathway could be the first step in the targeted therapy that might halt the development of hypertension in salt sensitive individuals, although current methods to treat such an issue have yet to be reliably demonstrated.

The understanding of the overall role of paraventricular nucleus magnocellular and parvocellular neurons remains somewhat ambiguous. Several studies have identified the role of the magnocellular neurons to be primarily neuroendocrine (3) with cells staining positively for oxytocin as well as vasopressin,

a hormone that has been historically associated with fluid balance. While we did observe a change in the *Fos* production in magnocellular neurons vs control after sodium treatment there was no significant difference between the two treatment groups, suggesting that magnocellular neurons likely play a negligible role in the G-protein gated sympathoinhibitory pathway that is of primary interest to this study. Parvocellular neurons appear to be involved in the normal sympathoinhibitory pathways that are activated in the presence of high salt (45). Studies have traced projections from the PVN to the MnPO as well as the IML (49) both areas understood to play important roles in sympathetic control of vasculature. Our own findings have shown that a peripheral sodium challenge increased *Fos* production in the PVN parvocellular neurons, as well as showing that down regulation of $G\alpha_{i2}$ significantly decreased this neural activation in response to salt.

Our overall findings suggest an important role for central $G\alpha_{i2}$ protein gated signal transduction in the normal presumably sympathoinhibitory response to increased sodium loading. These studies also help to illuminate that the body responds differently to increased sodium given peripherally (IV) as opposed to centrally (ICV). It was noteworthy that while in the peripheral study we saw an increase in the amount of time required for the $G\alpha_{i2}$ ODN pre-treated animals to return to normotension, there was no such difference found in the animals challenged centrally. Additionally it was found that natriuresis was attenuated in $G\alpha_{i2}$ ODN pre-treated animals that were challenged centrally, however, no such differences were seen in the renal excretory parameters for the animals that were challenged

peripherally. This finding is consistent with the idea of two different salt driven presumably sympathoinhibitory responses which work cooperatively in normally functioning rats, with the implications that any sort of malfunction in either system could potentially result in the development of salt sensitive hypertension. Important to this study is the idea that while central $G\alpha_{i2}$ protein pathways are vital to both central and peripheral responses to salt, it is possible that it is not the same $G\alpha_{i2}$ protein gated signal transduction pathways that are activated by each of the stimuli. This is illustrated by the differences seen in activation in PVN parvocellular neurons between the two treatment groups after a peripheral sodium load while such a difference is absent after a central sodium challenge. This could potentially be explained as evidence that the sympathoinhibitory $G\alpha_{i2}$ protein gated signal transduction pathway has been evolutionarily conserved as organisms have increased in neural complexity.

Clarity

The results of this study showed that it is possible to apply the CLARITY electrophoretic tissue clearing technique to larger organisms though whether or not it is possible to maintain the tissue integrity necessary for detailed studies of integrative systems involved in hypertension still remains unclear. Even given the limitations we encountered in our current studies the CLARITY technique or some form of it has already been utilized in number of other studies of complex neurological pathologies that include Alzheimer's disease (2), Multiple Sclerosis (43), and some pioneering studies in addiction behaviors (21).

Because of the relative novelty of the CLARITY method little has been published on the practice of clarifying large tissue and even less is posted about the use of CLARITY on rats, as a result we encountered several issues. One of the initial issues is that electrophoresis chambers designed for large volume tissue clearing are not yet commercially available and therefore have to be fabricated. There are a number of resources available with instructions for constructing small scale ETC chambers (48), however, most of these resources were intended for use with mice and not rats. We found that the important details related to chamber fabrication were that while the tissue needs to remain in the electric field for the best clearing result it can be highly detrimental if contact is made with either of the electrodes, so some steps should be taken to loosely secure the tissue in place. This serves a secondary function of protecting any sample from traumatic or abrasive effect of a constantly circulating solution. We found in early trials that leaving the tissue fully exposed to both the electrical field and the moving solution could slowly degrade the outer tissue that had already been cleared. The degradation of peripheral tissue presents some major issues to the study of hypertension since areas of the brain involved in body fluid homeostasis including the supra-optic nucleus are found peripherally. We used two cell IHC cell strainers caged together to hold the tissue in place as well as to provide a barrier from the electrodes, which helped to minimize tissue damage.

Another variable that we had some trouble with was the pH of the clearing solution. When the solution is initially prepared it is brought to a pH of 8.5, however, during the tissue clearing process acid can accumulate in the lipid mycelles lowering

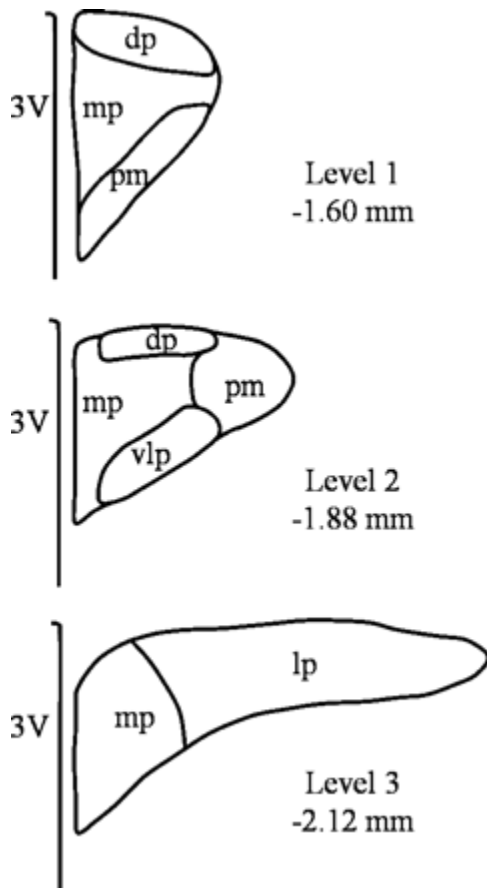
the pH of the circulating solution. Once the pH of the clearing solution falls below 7 it becomes ineffective at clearing the specimen and any further acidity can risk damaging the remaining tissue so close monitoring of the clearing solution is necessary for the best results. In our experiments we used a water circulator that held around 2 liters of solution, during the first trial we ran each sample to completion before changing the solution. We altered this protocol to include changing the solution every 3 days to account for the higher accumulation of acids given the significant increase in tissue volume as a result of switching animal species. Regular changing of the clearing solution proved highly beneficial to the tissue clearing process.

Degassing also presented a number of issues related to the new tissue size. Sample N1 was put under vacuum (-0.1atm) for a total of 10 min before addition of nitrogen gas. Due to the continued appearance of gas bubbles within the hydrogel after ten minutes sample N2 was kept under vacuum (-0.1atm) for a total of 20 minutes before the addition of nitrogen, although bubbling still occurred the number of bubbles was markedly diminished after additional time under vacuum. Samples N3 and N4 were both kept under vacuum for 30 min before introduction of nitrogen gas. Both samples N5 and N6 were placed under vacuum for 45 min before addition of nitrogen. Minimal bubbling was still evident at this point, however, continued time under vacuum was ruled out due to temperature constraints related to polymerization occurring if samples were allowed to warm to room temperature.

Overall we saw our best results with the tissue that was degassed under a vacuum for 45 min, followed by 7 days of ETC at 30V and 37°C, with a change of clearing solution after 3 and 6 days. Our results showed that the CLARITY method for optically clearing tissue as a means of tracking neuronal connections in intact specimens could plausibly be applied to the neural sympathoinhibitory pathway related to sodium dependent hypertension. Because of monetary and time restraints this study was not able to cover any of the staining or imaging protocols so further research will be necessary into the value of such a study but the early signs look promising.

APPENDIX

1.



Schematic drawings of 3 rostral-caudal levels of the hypothalamic paraventricular nucleus (PVN) that were sampled for analysis. *Level 1* was the most rostral and included the dorsal parvocellular, medial parvocellular, and ventrally located posterior magnocellular subnuclei. *Level 2* contained a prominent posterior magnocellular region and both dorsal and ventrolateral parvocellular divisions. *Level 3* was the most caudal and consisted of the medial and lateral parvocellular divisions. Coordinates are in reference to bregma using standard sections from the atlas of Paxinos and Watson (40). dp, dorsal parvocellular; mp, medial parvocellular; vlp, ventrolateral parvocellular; lp, lateral parvocellular; 3V, 3rd ventricle. Figure and caption taken from Stocker et. al. 2004 (44)

LIST OF JOURNAL

ABBREVIATIONS

Am J Physiol Regul Integr Comp Physiol	American Journal Physiology- Regulatory, Intergrative and Comparative Physiology
Acta Neuropathol	ACTA Neuropathologica
J Am Coll Cardiol	Journal of the American College of Cardiology
Curr Hypertens Rep	Current Hypertension Reports
Am J Physiol Heart Circ Physiol	American Journal of Physiology- Heart and Circulatory Physiology
J Physiol	Journal of Physiology

REFERENCES

1. Amin MS, Hong-Wei W, Reza E, Whitman SC, Tuana BS, and Leenen FH. Distribution of epithelial sodium channels and mineralcorticoid receptors in cardiovascular regulatory centers in rat brain. *Am J Physiol Regul Integr Comp Physiol* 289: R1787-R1797, 2005
2. Ando K, Laborde Q, Lazar A, Godefroy D, Youssef I, et. al. Inside Alzheimer brain with CLARITY: senile plaques, neurofibrillary tangles and axons in 3-D. *Acta Neuropathol* 128: 457-459, 2014
3. Antunes J, De Castro M, Elias L, Valenca M, and McCann S. Neuroendocrine Control of Body Fluid Metabolism. *Physiology Reviews* 84: 169-208, 2004
4. Antunes VR, Yao ST, Pickering AE, Murphy D, and Paton JFR. A spinal vassopressinergic mechanism mediates hyperosmolality- induced sympathoexcitation. *Journal of Physiology* 576.2: 569-583, 2006
5. Bahkis GL, Townsend RR, Liu M, Cohen SA, D'Agostino R, et. al. Impact of Renal Denervation of 24 Hour Ambulatory Blood Pressure: Results from Symplicity HTN-3. *J Am Coll Cardiol* 64(11): 1071-1078, 2014
6. Becker K, Jahrling N, Saghafi S, Weiler R, and Dodt H. Chemical clearing and dehydration of GFP expressing Mouse Brains. *PLoS ONE* 7(3): e33916, 2012
7. Bourque CW. Central mechanisms of osmoregulation and systemic osmoregulation. *Nature Reviews* 9:519-531, 2008

8. Campese VM, and Kogosov E. Renal Afferent Denervation Prevents Hypertension in Rats with Chronic Renal Failure. *Hypertension* 25: 878-882, 1995
9. Carey RM and Siragy HM. Newly recognized components of the renin-Angiotensin system: Potential roles in cardiovascular and renal regulation. *Endocrine Reviews* 24(3): 261-271, 2003
10. Cheong WF, Prael SA, and Welch AJ. A review of the optical properties of biological tissue. *IEEE Journal of Quantum Electronics* 26: 2166-2185, 1991
11. Chobain AV, Bakris GL, Black HR, Cushman WC, Green LA, et. al. Seventh report of the joint national committee on prevention, detection, evaluation, and treatment of high blood pressure. *Hypertension* 42: 1206-1252, 2003
12. Chung K, and Deisseroth K. Clarity for mapping the nervous system. *Nature Methods* 10: 508-513, 2013
13. Chung K, Wallace J, Kim SY, Kalyanasundaram S, Andalman AS, et al. Structural and molecular interrogation of intact biological systems. *Nature* 497: 332-337, 2013
14. Cunningham JT, Herreara-Rosales M, Martinez MA, and Mifflin S. Identification of Active Central Nervous System Sites in Renal Wrap Hypertensive Rats. *Hypertension* 49(2): 653-658, 2007
15. Fujita M, Ando K, Nagae A, and Fujita T. Sympathoexcitation by Oxidative Stress in the Brain Mediates Arterial Pressure Elevation in Salt-Sensitive Hypertension. *Hypertension* 50: 360-367, 2007

16. Fujita M, and Fujita T. The Role of CNS in Salt-sensitive Hypertension. *Curr Hypertens Rep* 15:390-394, 2013
17. Ganong W. Circumventricular organs: Definition and role in the regulation of endocrine and autonomic function. *Clinical and Experimental Pharmacology and Physiology* 27: 422-427, 2000
18. Gordon FJ, Haywood JR, Brody MJ, and Johnson AK. Effect of lesions of the Anteroventral Third Ventricle (AV3V) on the Development of Hypertension in Spontaneously Hypertensive Rats. *Hypertension* 4: 387-393, 1982
19. Hama H, Kurokawa H, Kawano H, Ando R, Shimogori T, et.al. Scale: A chemical approach for florescence imaging and reconstruction of transparent mouse brain. *Nature Neuroscience* 14: 1481-1488, 2011
20. Hindmarch C, Fry M, Yao ST, Smith PM, Murphy D, et. al. Microarray analysis of the transcriptome of the subfornical organ in the rat: regulation by fluid and food deprivation. *Am J Physiol Regul Integr Comp Physiol* 295: R1914-R1920, 2008
21. Hsiang H, Epp JR, Van Den Oever MC, Yan C, Rashid AJ, et al. Manipulating a “Cocaine Engram” in Mice. *The Journal of Neuroscience* 34(42): 14115-14127, 2014
22. Huang BS, Wang H, and Leenen F. Enhanced sympathoexcitatory and pressor responses to central Na⁺ in Dahl salt-sensitive vs. -resistant rats. *Am J Physiol Heart Circ Physiol* 281:H1881-H1889, 2001.

23. Huang C, Yoshimoto M, Miki K, and Johns EJ. The contribution of brain angiotensin II to the baroreflex regulation of renal sympathetic nerve activity in conscious normotensive and hypertensive rats. *The Journal of Physiology* 574: 597-604, 2006
24. Huang C, Yoshimoto M, Miki K, and Johns E. The contribution of angiotensin II to the baroreflex regulation of renal sympathetic nerve activity in conscious normotensive and hypertensive rats. *J Physiol* 574.2: 597-604, 2006
25. Kantzides A, and Badoer E. Fos, RVLM-projecting neurons, and spinally projecting neurons in the PVN following hypertonic saline infusion. *Am J Physiol Regul Integr Comp Physiol* 284: R945-R953, 2003
26. Kapusta DR, Pascale CL, Kuwabara JT, and Wainford RD. Central nervous system Galphai2-subunit proteins maintain salt resistance via a renal nerve-dependent sympathoinhibitory pathway. *Hypertension* 61: 368-375, 2013
27. Kapusta DR, Pascale CL, and Wainford RD. Brain heterotrimeric Galphai(2)-subunit protein-gated pathways mediate central sympathoinhibition to maintain fluid and electrolyte homeostasis during stress. *FASEB Journal : official publication of the Federation of American Societies for Experimental Biology* 26: 2776-2787, 2012
28. Kato K, Shirasaka T, Kunitake T, Hanamori T, and Kannan H. Participation of arterial baroreceptors input and peripheral vasopressin in the suppression of renal sympathetic nerve activity induced by central salt loading in

- conscious rats. *Journal of the Autonomic Nervous System* 76 (2-3): 83-92, 1999
29. Ke MT, Fujimoto S, and Imai T. SeeDB: A simple and morphology preserving optical clearing agent for neuronal circuit reconstruction. *Nature Neuroscience* 16: 1154-1161, 2013
30. Kim S, Chung K, and Deisseroth K. Light microscopy mapping of connections in the intact brain. *Trends in Cognitive Science* 17(12): 596-599, 2013
31. Kitano H. Systems Biology: A brief overview. *Science* 295: 1662-1665, 2002
32. Krum H, Schlaich M, Whitbourn R, Sobotka PA, Sadowski J, et al. Catheter-based renal sympathetic denervation for resistant hypertension: a multicentre safety and proof-of-principle cohort study. *Lancet* 373:1275-1281, 2009
33. Malpas S. Sympathetic Nervous System Overactivity and Its Role in the Development of Cardiovascular Disease. *Physiology Reviews* 90: 513-557, 2010
34. McKinley MJ, Allen AM, Burns P, Colvill LM, and Oldfield BJ. Interaction of circulating hormones with the brain: The roles of the subfornical organ and the organum vasculosum of the lamina terminalis. *Clinical and experimental pharmacology and physiology* 25: S61-S67, 1998
35. Miller R, and Loewy A. ENaC γ -expressing astrocytes in the circumventricular organs, white matter, and ventral medullary surface: Sites for Na⁺ regulation by glial cells. *Journal of Chemical Neuroanatomy* 53: 72-80, 2013

36. Miller R, Wang M, Gray P, Salkoff L, and Loewy A. ENaC-expressing neurons in the sensory circumventricular organs become *c-fos* activated following systemic sodium changes. *American Journal of Physiology Regulatory, Integrative and Comparative Physiology* 305: R1141-R1152, 2013
37. Marx V. Microscopy: seeing through tissue. *Nature Methods* 11(12): 1209-1214, 2014
38. Ong KL, Cheung B, Man YB, Lau CP, and Lam K. Prevalence, Awareness, Treatment, and Control of Hypertension among United States Adults 1999-2004. *Hypertension* 49: 69-75, 2007
39. Oldfield BJ, Bicknell Rj, McAllen RM, Weisinger RS, and McKinley MJ. Intravenous hypertonic saline induces Fos immunoreactivity in neurons throughout the lamina terminalis. *Brain Research* 561: 151-156, 1991
40. Paxinos G, and Watson C. The Rat Brain in Stereotaxic Coordinates. San Diego, CA: Academic, 1998
41. Randolph RR, Li Q, Curtis KS, Sullivan MJ, and Cunningham JT. Fos expression following isotonic volume expansion of the unanesthetized male rat. *The American journal of physiology* 274: R1345-1352, 1998
42. Simmonds SS, Lay J, and Stocker SD. Dietary Salt Intake Exaggerates Sympathetic Reflexes and Increases Blood Pressure Variability in Normotensive Rats. *Hypertension* 64: 583-589, 2014
43. Spence RD, Kurth F, Itoh N, MacKensie-Graham AJ, et. al. Bringing CLARITY to gray matter atrophy. *NeuroImage* (2014)

44. Stocker SD, Cunningham JT, and Toney GM. Water deprivation increases Fos immunoreactivity in PVN autonomic neurons with projections to the spinal cord and rostral ventrolateral medulla. *American journal of physiology Regulatory, integrative and comparative physiology* 287: R1172-1183, 2004
45. Stocker SD, Madden CJ, and Sved AF. Excess dietary salt intake alters the excitability of central sympathetic networks. *Physiology & Behavior* 100: 519-524, 2010
46. Stocker SD, Monahan KD, and Browning KN. Neurogenic and sympathoexcitatory actions of NaCl in hypertension. *Current hypertension Reports* 15: 538-546, 2013
47. Susaki EA, Tainaka K, Perrin D, Kishino F, Tawara T, et. al., Whole- Brain Imaging with Single-Cell Resolution Using Chemical Cocktails and Computational Analysis. *Cell* 157: 1-14 2014
48. Sulkin MS, Widder E, Shao C, Holzem KM, Gloschat C, et. al. Three-dimensional printing physiology laboratory technology. *Am J Physiol Heart Circ Physiol* 305: H1569–H1573, 2013.
49. Swanson LW and Sawchenko PE. Paraventricular Nucleus: A site for the integration of neuroendocrine and autonomic mechanisms. *Neuroendocrinology* 31: 410-417
50. Symplicity HTN-1 Investigators. Catheter-Based Renal Sympathetic Denervation for Resistant Hypertension, Durability of Blood Pressure Reduction Out of 24 Months. *Hypertension* 27: 911-917, 2011

51. Wainford RD, Carmichael CY, Pascale CL, and Kuwabara JT. Galpha₂-Protein-Mediated Signal Transduction: Central Nervous System Molecular Mechanism Countering the Development of Sodium-Dependent Hypertension. *Hypertension* 65: 178-186, 2015
52. Wainford RD, and Kapusta DR. Functional selectivity of central Galpha-subunit proteins in mediating the cardiovascular and renal excretory responses evoked by central alpha(2) -adrenoceptor activation in vivo. *British Journal of Pharmacology* 166: 210-220, 2012
53. Wainford RD, and Kapusta DR. Hypothalamic paraventricular nucleus G alpha q subunit protein pathways mediate vasopressin dysregulation and fluid retention in salt- sensitive rats. *Endocrinology* 151: 5403-5414, 2010
54. Wainford RD, Pascale CL, and Kuwabara JT. Brain Galpha₂-subunit protein-gated pathways are required to mediate the centrally evoked sympathoinhibitory mechanisms activated to maintain sodium homeostasis. *Journal of Hypertension* 31: 747-757, 2013
55. Watanabe E, Hiyama TY, Shimizu H, Kodama R, Hayashi M, et al. Sodium-level-sensitive sodium channel Na_x is expressed in glial laminae processes in the sensory circumventricular organs. *Am J Physiol Regul Integ Comp Physiol* 290: R568-R576, 2006
56. Weinberg M. Pathogenesis of salt sensitivity of blood pressure. *Current Hypertension Reports* 8.2: 166-170, 2006

57. Weinberger MH, Fineberg NS, Fineberg SE, and Weinberger M. Salt Sensitivity, Pulse Pressure, and Death in Normal and Hypertensive Humans. *Hypertension* 37(2): 429-432, 2001
58. Xu Z, and Herbert J. Regional suppression by lesions in the anterior third ventricle of *c-fos* expression induced by either angiotensin II or hypertonic saline. *Neuroscience* 67, 1: 135-147, 1995
59. Yang B, Treweek JB, Kuljarni RP, Deverman BE, Chen CK, et. al. Single-Cell Phenotyping within Transparent Intact Tissue through Whole Body Clearing. *Cell* 158: 1-14, 2014

Curriculum Vitae

Christopher Matthew Neal

Cmatthewstand@gmail.com

16002 Marjan Ln, Huntington Beach, CA, 92647

EDUCATION

MS, Medical Science

August 2013- May 2015

Boston University School of Medicine, Division of Graduate Medical Sciences

BS, Biology with option in Physiology, Chemistry minor

September 2005- December 2011

California State University at Long Beach

High School Graduate with Honors

September 2001- June 2005

Marina High School, Huntington Beach, CA

WORK EXPERIENCE

Pathology Lab Assistant – July 2012- July 2013

Hoag Hospital Pathology

Newport Beach, CA

Primary responsibilities:

- Accessioning pathology and cytology specimens brought into lab
- Preparing frozen sections for pathologists to view
- Communicating with other departments or doctors' offices to clarify issues
- Answering phones, cleaning, restocking, filing and other assorted office keeping
- Sending out specimens for additional testing

Nutrition Assistant – February 2007- January 2011

Nutrition Assistant Lead- Jan 2011- July 2012

Hoag Hospital

Newport Beach, CA

Primary responsibilities:

- Organizing team of nutrition assistants to meet daily workflow needs
- Supervising the trayline during meal times
- Addressing issues arising with the other nutrition assistants
- Taking future meal orders for patients that are consistent with the prescribed diet orders
- Delivering and picking up meals
- Cleaning, and stocking refrigerators in each of the nursing units throughout the hospital

Office Assistant- October 2003- January 2006

HB Digital Reprographics and Imaging
Huntington Beach CA

Primary responsibilities:

- Making copies of blueprints using a large format copier and scanner
- Answering phones, cleaning, helping customers, other office related side work
- Delivering products to clients offices

Volunteer Experience

Boston Healthcare for the Homeless, Case Management volunteer

Barbara McGinnis House
Boston MA

Primary responsibilities:

- Helping patients to attain new ID, Social Security cards, Food stamps, and phones
- Assisting patients with filling out forms
- Assisting patients in attending medical appointments, legal appointments as well as apartment viewings in government subsidized areas
- Doing psycho-social entrance interviews
- Helping patients run everyday errands

Eagle Scout

Huntington Beach, CA, 2003